Journal of Neural Engineering

Automated detection of ripple oscillations in long-term scalp EEG from patients with infantile spasms

To cite this article before publication: Colin Matthew McCrimmon *et al* 2020 *J. Neural Eng.* in press https://doi.org/10.1088/1741-2552/abcc7e

Automated Detection of Ripple Oscillations in Long-Term Scalp EEG from Patients with Infantile Spasms

Colin M. McCrimmon[1,2], Aliza Riba[3], Cristal Garner[3], Amy L. Maser[4], Donald J. Phillips[3,5] Maija Steenari[3,5] Daniel W. Shrey[3,5], Beth A. Lopour[6*]

1 Medical Scientist Training Program, University of California, Irvine, CA 92617, USA
2 Dept. Neurology, University of California, Los Angeles, CA 90095, USA
3 Div. Neurology, Children's Hospital of Orange County, Orange, CA 92868, USA
4 Dept. Psychology, Children's Hospital of Orange County, Orange, CA 92868, USA
5 Dept. Pediatrics, University of California, Irvine, Irvine, CA 92617, USA
6 Dept. Biomedical Engineering, University of California, Irvine, Irvine, CA 92617, USA
* beth.lopour@uci.edu

Abstract

Objective: Scalp high frequency oscillations (HFOs) are a promising biomarker of epileptogenicity in infantile spasms (IS) and many other epilepsy syndromes, but prior studies have relied on visual analysis of short segments of data due to the prevalence of artifacts in EEG. Here we set out to robustly characterize the rate and spatial distribution of HFOs in large datasets from IS subjects using fully automated HFO detection techniques.
Methods: We prospectively collected long-term scalp EEG data from 12 subjects with IS and 18 healthy controls. For patients with IS, recording began prior to diagnosis and continued through initiation of treatment with adenocorticotropic hormone (ACTH). The median analyzable EEG duration was 18.2 hours for controls and 84.5 hours for IS subjects (∼1300 hours total). Ripples (80-250 Hz) were detected in all EEG data using an automated algorithm.
Results: HFO rates were substantially higher in patients with IS compared to controls. In IS patients, HFO rates were higher during sleep compared to wakefulness (median 5.5/min and 2.9/min, respectively; p =0.002); controls did not exhibit a difference in HFO rate between sleep and wakefulness (median 0.98/min and 0.82/min, respectively). Spatially, IS patients exhibited significantly higher rates of HFOs in the posterior parasaggital region and significantly lower HFO rates in frontal channels, and this difference was more pronounced during sleep. In IS subjects, ACTH therapy significantly decreased the rate of HFOs.
Discussion: Here we provide a detailed characterization of the spatial distribution and rates of HFOs associated with infantile spasms, which may have relevance for diagnosis and assessment of treatment response. We also demonstrate that our fully automated algorithm can be used to detect HFOs in long-term scalp EEG with sufficient accuracy to clearly discriminate healthy subjects from those with IS.

Introduction

Infantile spasms (IS) are associated with developmental delay and an electroencephalographic (EEG) pattern known as hypsarrhythmia, and this triad of symptoms is referred to as West syndrome [1]. IS carries a poor prognosis, as spasms may evolve into persistent neurological deficits, intractable seizures, and Lennox-Gastaut syndrome, and they carry an increased mortality risk [2,3]. Not only are these outcomes devastating to patients' families, but they also put a tremendous burden on the already-strained U.S. healthcare system [3]. Because early treatment initiation may positively impact outcomes [3–5], prompt diagnosis is crucial. However, prolonged video-EEG monitoring is often required to capture epileptic spasms and ictal events. Moreover, the classically associated interictal EEG pattern known as hypsarrhythmia (high amplitude asynchronous slow waves with multifocal spikes and polyspikes [6]), may not be present [6–8] or may have highly variable features [9,10], leading to poor inter-rater reliability for its identification [11,12]. Thus, discovery of other salient spasms-associated EEG features is imperative to facilitate prompt and accurate diagnosis.

One such feature may be interictal cortical high-frequency oscillations (HFOs). HFOs are electrographic events with a peak frequency above 80 Hz, corresponding to oscillations in the ripple band (80-200 Hz) and fast ripple band (200-500 Hz), as well as to the upper end of the gamma band (∼60-200 Hz) [13]. In healthy individuals, the information encoded in these frequencies are thought to play a role in diverse cortical processes, such as sensory processing, memory consolidation, attention, and movement planning/control [14–17]. In patients with epilepsy, HFOs are thought to be temporally associated with ictal events [18, 19] and are also spatially associated with seizure onset zones [20, 21]. In fact, even interictal HFOs may spatially correlate with seizure onset zones [22–24] and may be useful in predicting long-term outcomes of epilepsy surgery [25].

Many studies support that EEG is a reliable, noninvasive modality to study scalp HFOs in the ripple [26–29] and fast ripple frequency bands [30–32]. Studies using simultaneous scalp and intracranial EEG have confirmed that scalp-visible oscillations have neural origin [29–31]. Scalp HFOs have been associated with various pediatric epilepsies, including benign epilepsy with centrotemporal spikes [33], epileptic encephalopathy with continuous spike-and-wave during sleep [34, 35], idiopathic partial epilepsy of childhood [36], tuberous sclerosis complex [32], and myoclonic seizures [37]. Visual detection is standard in such studies, due to the pervasive nature of scalp EEG artifacts. However, semi-automated detection methods have been proposed in which candidate HFOs are identified via an automated algorithm and all detections are visually reviewed to reject false positives [29, 32, 33, 38]. von Ellenrieder et al. (2012) created a fully automated detection method, but they recommended expert review of detected events [28]. Our group also published a fully automated method for detection of scalp HFOs, but it was applied to a small dataset (∼10 minutes of data per subject) [39].

HFOs in the gamma and ripple bands have also been reported during epileptic spasms using ictal scalp EEG [18–20, 40, 41]. In some cases, the HFOs were found to be focal, despite the visual appearance of a generalized spasm onset [19, 40]. Fewer studies have examined HFOs in IS using interictal data. One study [38] analyzed both ictal and interictal HFOs in patients with IS without focal features in hypsarrhythmia, and they compared the results to scalp EEG from normal control subjects. They found higher rates of interictal HFOs in the gamma and ripple frequency bands in patients with West Syndrome, and the occurrence of HFOs decreased following treatment with ACTH. A second study found that beta and gamma scalp oscillations were more frequently associated with IS compared to other pediatric epilepsies [22]. However, these studies only utilized a few minutes of interictal data for each subject, given the time-intensive nature of visually identifying HFOs, and thus the generalizability of their findings remains limited.

Therefore, we sought to further characterize interictal HFOs in patients with IS using long-term recordings and fully automated methods. We measured scalp EEG in normal controls and patients with IS, performed automatic detection of HFOs, and compared the following: 1) the rates of HFOs during wakefulness and sleep, 2) the spatial distribution of HFOs across the scalp, and 3) the effect of treatment initiation on HFO rate.

Methods

Subject Recruitment

This prospective longitudinal study was approved by the Children's Hospital of Orange County (CHOC) Institutional Review Board. Children aged 0-3 years who were admitted to the hospital for long-term video EEG monitoring with concern for new onset epileptic spasms were approached for informed parental consent. Subjects with a previous diagnosis of infantile spasms and those who had been previously treated with adrenocorticotropic hormone (ACTH) or vigabatrin (VGB) were excluded from the study. It should be emphasized that long-term video EEG monitoring was performed solely based on clinical suspicion for IS and was in no way influenced by our study. The developmental status of each subject was evaluated by a board-certified neuropsychologist (Amy Maser, PhD) using the Vineland Adaptive Behavior Scales, Third Edition [42].

Video-EEG Monitoring

Subjects underwent continuous video EEG monitoring while being recorded with 19 scalp electrodes placed according to the international 10-20 system [43] and two mastoid reference electrodes. Data from these electrodes were

simultaneously acquired at 5 kHz for the research study and at 200 Hz for clinical monitoring, using a Neurofax EEG-1200 acquisition system with JE-120A amplifier fitted with a QI-124A dual data stream recording unit (Nihon Kohden, Tokyo, Japan). Electrooculographic (EOG), electromyographic (EMG), and electrocardiographic (ECG) data were also acquired at 5 kHz and 200 Hz using the same system. Note that EMG electrodes were positioned over the masseter muscles in all subjects. The initial recording duration for each subject was overnight (approximately 18-24 hours), at which time a board-certified pediatric epileptologist reviewed the video-EEG data for clinical evidence of IS. Control subjects were defined as those who had (1) no known neurological diseases, (2) no abnormal neuroimaging, (3) normal video EEG recordings with the events of concern captured, and (4) normal scores on the Vineland-3. Subjects with evidence of IS who were started on ACTH (first-line therapy) were assigned to the IS group and continued to undergo continuous video-EEG monitoring for an additional 48-96 hours using the aforementioned study and clinical data acquisition parameters. An IS subject was designated as a "responder" if they exhibited cessation of clinical spasms and their EEG no longer met criteria for hypsarrhythmia (defined as high amplitude (>200 microvolt), continuous arrhythmic delta activity with multifocal independent epileptiform discharges and lack of normal background activity) during a follow-up overnight video EEG recording performed approximately 2 weeks after their initial IS diagnosis was made. "Non-responders" had persistent spasms and/or hypsarrhythmia at follow-up.

Analysis

All study data were processed using the same custom MATLAB (The MathWorks, Natick, MA) software. This software: 1) removed amplifier saturation (clipping) artifacts from the dataset, 2) re-referenced the remaining signals to a longitudinal bipolar montage [44], 3) performed candidate HFO detection as described in [45]. Briefly, initial HFO detection involved applying an infinite impulse response (IIR) band-pass filter (80-250 Hz, 10th order) and rectifier to the data, and then identifying any high-amplitude oscillations, i.e. $\geq$3 consecutive oscillations with amplitude greater than the upper-limit of background high-gamma activity (defined as the gamma cumulative distribution function from the surrounding 5s of data with α=0.0001). While finite impulse response (FIR) filters are typically preferred, IIR filters drastically reduce computation time and have been used successfully for HFO analysis [46]. We chose the IIR filter settings by visually confirming the similarity to data filtered with the equivalent FIR filter. We then applied additional criteria to the candidate events to reject false positive detections; note that the steps used here differ from our previous algorithm developed for scalp EEG [39]. Here, any HFOs with corresponding electrode "pop" artifacts [47] (defined as DC shifts >50 μV) or muscle artifacts (defined as line length >1900 with units $\sqrt{\mu V^2 + s^2}$) within a 0.3-second sliding window from the longitudinal-bipolar-referenced signals were discarded. Analysis of the larger, 0.3-second window helped identify longer periods of muscle artifact, as candidate events were frequently detected at the onset and offset of this high amplitude activity. Note that the voltage and line length cutoffs were empirically determined from a very small subset of the data by visually inspecting the candidate HFOs detected as above and manually modifying the cutoffs to reject apparent "pop" and muscle artifacts while preserving true HFOs. The subsequent optimal cutoffs were then applied to the remaining dataset.

HFO Detection Validation

After events were automatically detected in all subjects, a visual validation procedure was completed using HFOs, high-frequency artifacts (initially classified as HFOs but rejected via the DC shift and line-length cutoffs), and background EEG (the remaining data). For control subjects, an automated script randomly selected 25 examples of each type of signal (HFOs, artifacts, background EEG) based on the automated HFO detection results. Similarly, this automated script randomly selected 50 examples of each type of signal based on the automated HFO detection results from the data of each IS subject. The broadband and ripple-band filtered data associated with each of these examples (with surrounding 1s of data) were presented to two trained human reviewers for manual classification. Events were displayed in a random order, and reviewers were blinded to the results of the automated HFO detection.

HFO Rates

To compare HFO rates in spasms subjects versus control subjects, the total number of HFOs per minute summed across all electrodes was calculated for each subject. Note that in this analysis, to avoid overcounting HFOs with long durations or single HFOs captured by multiple channels (e.g. via volume conduction), any HFO that occurred <1 second after a previous HFO (even from a different channel) was discarded. Manual EEG sleep staging was performed for all control subject studies by a registered polysomnographic technologist (Cristal Garner, REEGT, RPSGT) in accordance with the American Academy of Sleep Medicine (AASM) guidelines. Manual sleep staging was

not possible for IS subjects given the size of the datasets and the unreliability of manual sleep staging in this patient population due to epileptic spasms and hypsarrhythmia altering sleep stage structure and progression [48–51]. However, by generating a classifier from EOG, EMG, and ECG data in the control subjects, we were able to mark periods of sleep and wakefulness in IS subjects solely from these non-EEG signals that are likely just as reliable in IS subjects as in control subjects. Briefly, this classifier utilized linear discriminant analysis [52] for dimensionality reduction of the EOG, EMG, and ECG data, followed by a Bayesian classifier using a Gaussian likelihood model. A Wilcoxon rank-sum test [53] was used to compare the HFO rates between control subjects and IS subjects during wakefulness and during sleep. A Wilcoxon signed-rank test for paired data [54] was used to compare the HFO rates during wakefulness and sleep for control and IS subjects. Note that for these analyses, HFO rates were calculated from the entirety of the IS subject recordings including pre- and post-ACTH data.

Spatial Distribution of HFOs

To compare the spatial distribution of HFOs throughout the scalp in control and IS subjects, we calculated the number of HFOs per minute at each electrode for every subject during wakefulness and sleep. Note that unlike above, HFOs that occurred <1 second after a previous HFO from a different channel were not discarded in this analysis. This ensured that the spatial distribution of each event was accurately represented; if an event occurred simultaneously in two channels, we counted the event for both channels, rather than arbitrarily removing it from one of them. Lastly, to compare the distributions across subjects, the HFO rate from each electrode was normalized by dividing by the sum of HFO rates across all electrodes for that subject. Multiple Wilcoxon rank-sum tests were used with a Bonferroni correction (α =0.05/N, where the number of channels N=18) to determine which channels exhibited a significant difference in HFO rates between IS and control subjects.

HFO Rates Before and After ACTH Initiation

A Wilcoxon signed-rank test was used to compare HFO rates prior to and >24 hours after initiating ACTH therapy in IS subjects while awake and asleep. Note that each pair consisted of one patient's HFO rate during either wakefulness or sleep (summed across all electrodes while avoiding overcounting, as described in the *HFO Rates* section above), and the two samples of EEG were clipped as follows: 1) from the start of video-EEG monitoring to the first dose of ACTH, and 2) from 24 hours after the first dose of ACTH to the completion of video-EEG monitoring.

Results

Subject Enrollment/Video-EEG Monitoring

Thirty-one subjects were enrolled in the study from January 2017 through February 2019 and contributed ∼1300 total hours of analyzable EEG data. Eighteen subjects were assigned to the control group (4 males, median age 6.7 months, lower quartile 3.0 months, upper quartile 8.2 months). Median usable recording duration was 18.2 hours (lower quartile 16.3 hours, upper quartile 20.9 hours). For all control subjects, the events of interest were captured on video EEG and found to not resemble epileptic spasms. All of the control subjects' EEG studies were within normal limits for age with no slowing, epileptiform discharges, nor seizures noted. Only one control subject (subject 4) had neuroimaging (MRI) performed, and it was within normal limits. All control subjects had Vineland-3 developmental scores within normal limits (greater than 85). The classifier that used EOG, EMG, and ECG data to predict wake and sleep states for IS subjects was generated from the control subjects' data and had a mean leave-one-out cross-validation accuracy of 86% when compared with the manual sleep staging results for control subjects. Note that EKG data from control subject 17 had significant artifacts that, for unclear reasons, were present predominantly while the patient was sleeping. These artifacts contributed to a clearly erroneous anticorrelation between the processed EKG data and the other sensor data (EMG, EOG), along with poor cross-validation performance (40%), so the processed EKG data was inverted prior to the dimensionality reduction step, which substantially improved the cross-validation performance (90%).

Thirteen of the thirty-one enrolled subjects demonstrated epileptic spasms (IS group) during video-EEG monitoring (4 males, median age 8.1 months, lower quartile 6.9 months, upper quartile 14.4 months). Note that one IS subject was briefly enrolled in the study, but was prematurely withdrawn by her parents only 3 hours and 40 minutes after starting EEG monitoring; she is not included in our analysis or mentioned elsewhere in this manuscript. The median

recording duration of the remaining 12 IS subjects included in this study was 84.6 hours (lower quartile 56.9 hours, upper quartile 110.9 hours). Clinical data for these subjects are shown in Table 1. This group included individuals with genetic syndromes (trisomy 21, CDKL5, 2q24 and 2p24 deletion, 5q deletion) as well as those with a history of occipital lobe epilepsy, intracranial hemorrhage with gliosis, and sinus venous thrombosis. IS subject 1 was on phenobarbital and levetiracetam at the start of the study. IS subject 4 was on phenobarbital at the start of the study. IS subject 5's video-EEG monitoring was discontinued ∼14 hours after the initiation of ACTH therapy. IS subject 9 was initially diagnosed with focal seizures and was started on Phenobarbital, however, clinical follow-up with a subsequent video EEG captured epileptic spasms as well, and the patient was started on ACTH therapy 1 month after the initial video-EEG monitoring. Due to technical difficulties, only ∼2 hours of data was recorded from IS subject 10 at the study-specified acquisition rate (5 kHz) before the subject started ACTH therapy, but the clinical recording was unaffected. Also note that subject 10 was prescribed levetiracetam at the study onset. IS subject 12 only participated in the initial ∼24 hours of video-EEG monitoring and was started on ACTH therapy immediately after. Still, in total, ∼1300 hours of EEG data were analyzed, and >900,000 HFOs were detected.

Analysis

Epileptic Spasms in IS Subjects

Board-certified pediatric epileptologists (DJP, DS, MS) reviewed ∼12-hour-long samples of video-EEG data from each IS subject and documented every epileptic spasm. A total of 1085 epileptic spasms were recorded (17, 215, 164, 34, 90, 85, 173, 31, 2, 135, 23, 116 from IS subjects 1-12, respectively). Note that subject 9 had minimal events (2) during the reviewed 12-hour-long sample and was formally diagnosed with IS during a subsequent follow-up study. The observed epileptic spasms tended to cluster temporally (as many as 9 events within 1 minute time for subject 1), and typically occurred at night and early in the morning. Of the 1085 documented spasms, 616 (57%) occurred within 1 second of a potential HFO (before artifact rejection based on voltage and line length cutoffs described above), and only 335 (31%) occurred within 1 second of a detected HFO. Therefore, given the short duration of each spasm, there are a small number of potentially ictal HFOs in these 12-hour samples. It can be concluded by extrapolation that the vast majority of the >900,000 HFOs detected in this study were interictal.

HFO Detection Validation

The ability of the automated HFO detection algorithm to discriminate between HFOs, high-frequency artifacts (including sharp transients, "pops", DC shifts, muscle), and background EEG was compared to manual classification by two trained human reviewers, and the results are provided in Supplementary Figure 1. Briefly, the two reviewers agreed on the class (HFO, artifact, background EEG) of the signals presented to them ∼86% of the time. Note that the reviewers were largely consistent with each other (>90%) when identifying background EEG and high-frequency artifacts but were less consistent with each other in their classification of HFOs (75% for control cases and 69% for IS cases). For the control subjects, most of the signals classified as HFOs by automated HFO detection were classified by the reviewers as high-frequency artifacts, and only 13% and 28%, respectively, were classified as true HFOs by Reviewers 1 and 2. For the IS subjects, 51% and 59%, respectively, of the signals classified as HFOs by automated HFO detection were classified as true HFOs by Reviewer 1 and 2. For the control subjects, Reviewers 1 and 2 thought that 91% and 94%, respectively, of the automatically-classified high-frequency artifacts were correctly identified. For the IS subjects, the numbers were similar at 92% and 91%, respectively. For the control subjects, Reviewers 1 and 2 thought that 97% and 94%, respectively, of the signals that were automatically classified as background EEG were correctly identified. For the IS subjects, the numbers were similar at 96% and 93%, respectively.

HFO Rates

As depicted in Figure 1, the median HFO rate for the control subjects was 0.82/min while awake and 0.98/min while asleep, and the median HFO rate for IS subjects was 2.9/min while awake and 5.5/min while asleep. HFO rates during both wakefulness and sleep were significantly increased in IS subjects compared to control subjects per Wilcoxon rank-sum tests (both $p < 0.0001$). Note that these results did not change (both $p < 0.0001$) when a leave-one-out automated wake/sleep classifier was used for the control subjects rather than manual wake/sleep classification. HFO rates for the control subjects when an automated wake/sleep classification was used are shown in Supplementary Figure 2. For IS subjects, there was a significant increase in the HFO rate while asleep compared to while awake ($p < 0.01$), per a Wilcoxon signed-rank test for paired data. For control subjects, there was no significant difference between the HFO rates while asleep and while awake ($p = 0.20$ using manual wake/sleep classification,

Subject	Age (mo) Sex	Pre-existing Epilepsy	AEDs at Study Onset	Video-EEG Results	Recording Duration (hr)	HFO Rate (Awake/Sleeping)	Response to ACTH
1	19.5 M	Y	Y	Epileptic spasms in clusters Hypsarrhythmia, esp. posteriorly Moderate-severe diffuse background slowing	87.0	2.2 (2.2/2.3)	N
2	8.7 M	N	N	Epileptic spasms in clusters Intermittent hypsarrhythmia Intermittent normal background	85.2	5.5 (3.1/6.7)	N
3	9.0 F	N	N	Epileptic spasms in clusters Hypsarrhythmia Severe diffuse background slowing	83.9	3.2 (2.6/3.4)	N
4	17.2 F	Y	Y	Epileptic spasms in clusters Hypsarrhythmia, esp. posteriorly Moderate-severe diffuse background slowing	113.5	4.7 (3.3/5.6)	Y
5	6.5 F	N	N	Epileptic spasms in clusters Hypsarrhythmia, esp. posteriorly Severe diffuse background slowing	65.8	4.8 (2.9/5.8)	N
6	5.9 F	N	N	Epileptic spasms in clusters Hypsarrhythmia Severe diffuse background slowing	71.2	4.3 (3.7/4.6)	N
7	11.5 F	N	N	Epileptic spasms in clusters Hypsarrhythmia Severe diffuse background slowing	113.0	13.4 (9.1/17.1)	N
8	18.0 F	N	N	Epileptic spasms in clusters Hypsarrhythmia, esp. right-posterior Diffuse background slowing, max right-posterior	111.9	6.2 (4.7/6.9)	Y
9	7.4 F	N	N	Back arching, likely spasms in clusters Hypsarrhythmia w/ focal R>L parasagittal discharges Moderate diffuse background slowing	15.2	2.9 (2.8/3.0)	Y
10	7.3 M	Y	Y	Epileptic spasms in clusters Hypsarrhythmia Severe diffuse background slowing	48.0	6.0 (3.0/7.6)	N
11	7.5 M	N	N	Epileptic spasms in clusters Hypsarrhythmia Severe diffuse background slowing	109.9	1.3 (1.8/1.0)	N
12	5.9 F	N	N	Epileptic spasms in clusters Modified hypsarrhythmia (less than 300 μV) Moderate diffuse background slowing	23.2	4.0 (1.5/5.5)	Y

Table 1. IS subjects' baseline and study characteristics. HFO rates are provided in units of min^{-1}. AEDs = antiepileptic drugs, ACTH = adrenocorticotropic hormone.

p =0.09 using automated wake/sleep classification).

Spatial Distribution of HFOs

As depicted in Figures 2 and 3, HFOs in the control subjects typically occurred outside of the posterior parasagittal region corresponding to bipolar signals from C3-P3, P3-O1, Fz-Cz, Cz-Pz, P4-O2, C4-P4 (the center column of channels outlined in these figures). The HFO rates had an otherwise broad distribution both while awake and during sleep, although the trend is more striking during sleep. In contrast, most of the HFOs in IS subjects during wakefulness and sleep were concentrated in a few channels, and these channels tended to include rather than spare the posterior parasagittal region. These comparisons can be seen clearly in Figure 4, which depicts the median spatial distribution of HFOs across control subjects and IS subjects while awake and asleep. Note that Figure 4 also displays the results of the Wilcoxon rank-sum tests (with Bonferroni correction), indicating that IS subjects have higher HFO rates in all posterior parasaggital channels and lower HFO rates in frontal channels, when compared to control subjects ($p < 0.01$).

HFO Rates Before and After ACTH Initiation

Figure 5 depicts the HFO rates before ACTH initiation and >24 hours after the first dose of ACTH. In the 8 IS subjects included in this analysis, there was a significant decrease in HFO rates during sleep after ACTH was started (p <0.01) per a Wilcoxon signed-rank test, with the median HFO rate across subjects decreasing from 6.8/min to 3.9/min. This was not true when patients were awake (p =0.11), with median HFO rate across subjects increasing from 2.5/min to 4.2/min. Note that of the three subjects with the largest ACTH-associated decrease in HFO rate during sleep (i.e. IS subjects 4, 6, and 8), two also exhibited a clinical response to ACTH therapy (see below). Recall that for this analysis, Subject 9 was excluded as she was initially diagnosed with focal epilepsy and started on phenobarbital, and Subjects 5, 10, and 12 were excluded because their pre- or post-ACTH study datasets were too small.

Four out of the twelve IS subjects (namely subjects 4, 8, 9, 12) initially responded clinically to ACTH therapy, and have been followed longitudinally since enrollment in the study. After ACTH initiation, the visual appearance of Subject 4's EEG did not change substantially, although possibly contained slightly fewer discharges. She has had no evidence of IS relapse to-date, although she has had other non-IS-related seizures and her EEG continues to have discharges. Subject 8 exhibited moderate improvement in discharges on EEG by the end of the study. However, she relapsed about 6 months later and continues to have discharges on EEG. Subject 9 did exhibit improvement in discharges on her EEG with initial phenobarbital therapy for what was thought to be focal epilepsy. However, when she was diagnosed with IS approximately one month later, ACTH therapy was initiated and she responded well with no evidence of IS relapse to-date. Due to the short clinical and non-clinical recording duration for Subject 12, it was not possible to evaluate fully for EEG changes, although her subsequent EEG appears to have normalized, and we are unaware of any relapse. Note that all non-responders exhibited no substantial EEG changes after ACTH initiation except for Subject 6, who demonstrated improved spike frequency and amplitude by the end of the study, and Subject 10, who demonstrated more generalized EEG improvements by the end of the study.

Discussion

This prospective study demonstrates fully automated detection of HFOs in long-term scalp EEG recordings and provides new insight into the characteristics of interictal scalp ripples in infants with IS. Patients with IS exhibited higher HFO rates than normal infant control subjects, and the rates were higher during sleep compared to wakefulness. In contrast, HFO rates for control subjects did not vary significantly across the sleep-wake cycle. Spatially, the distinction between the two groups was greatest in the posterior parasaggital region. HFOs in this region were frequently detected for IS subjects but rarely for control subjects, especially during sleep. ACTH therapy significantly and universally decreased HFOs in IS subjects during sleep, and the extent of this decrease tended to be large in subjects who clinically responded to treatment.

Our results are consistent with prior HFO studies using intracranial EEG. Based on these studies, it has become commonly accepted that interictal HFOs occur more frequently during sleep [55–57], although the difference is not always statistically significant [58, 59]. Bagshaw et al. [60] found similar diurnal HFO fluctuations in patients with focal epilepsy using implanted electrodes. The invasive nature of these measurements typically precludes analysis of

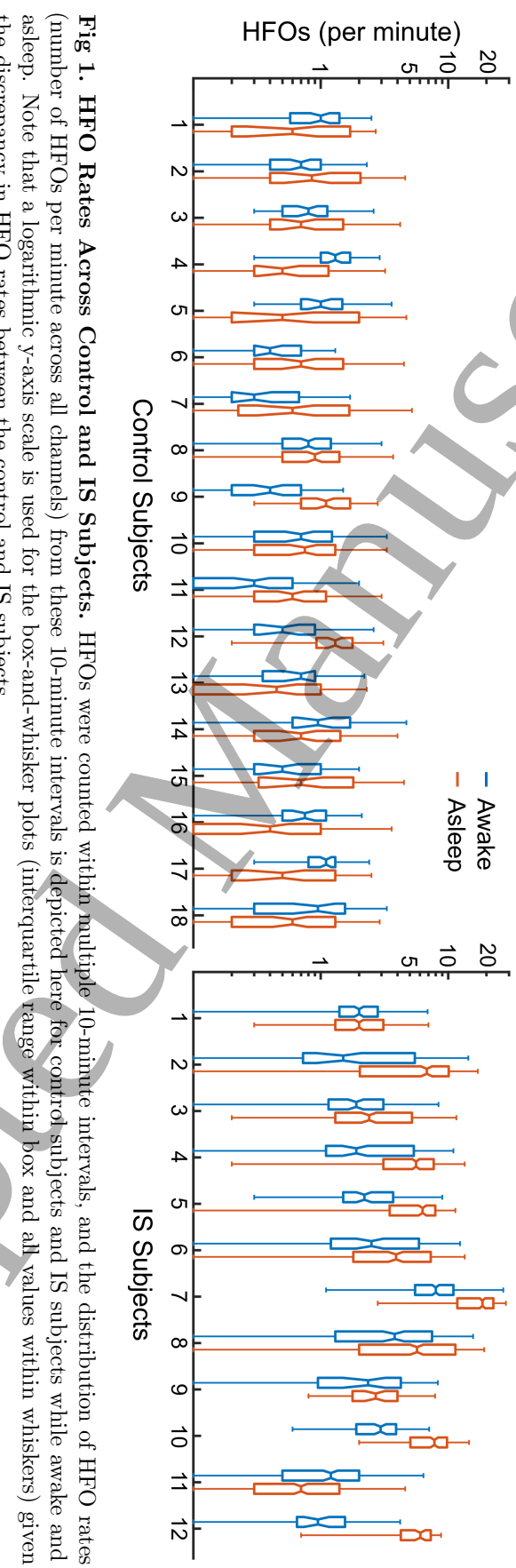

Fig 1. HFO Rates Across Control and IS Subjects. HFOs were counted within multiple 10-minute intervals, and the distribution of HFO rates (number of HFOs per minute across all channels) from these 10-minute intervals is depicted here for control subjects and IS subjects while awake and asleep. Note that a logarithmic y-axis scale is used for the box-and-whisker plots (interquartile range within box and all values within whiskers) given the discrepancy in HFO rates between the control and IS subjects.

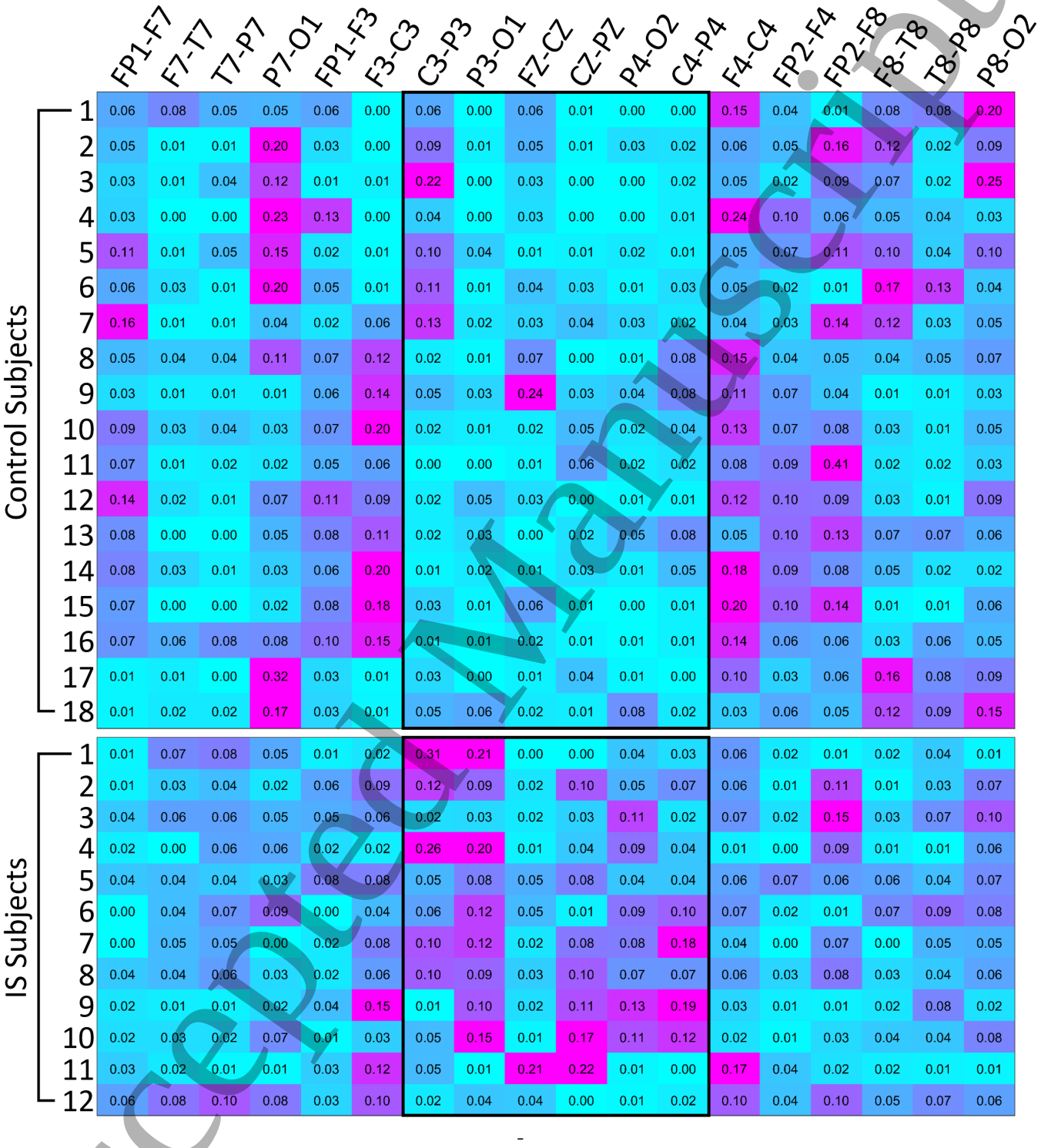

Fig 2. Normalized HFO Rates for Each Channel During Wakefulness. Each row represents a control or IS subject and each column corresponds to a channel from a longitudinal bipolar montage. HFO rates are normalized across each subject such that the sum of each row is 1.0, and higher rates appear pink while lower rates appear cyan. The channels contained in the black outlines correspond to posterior parasagittal areas.

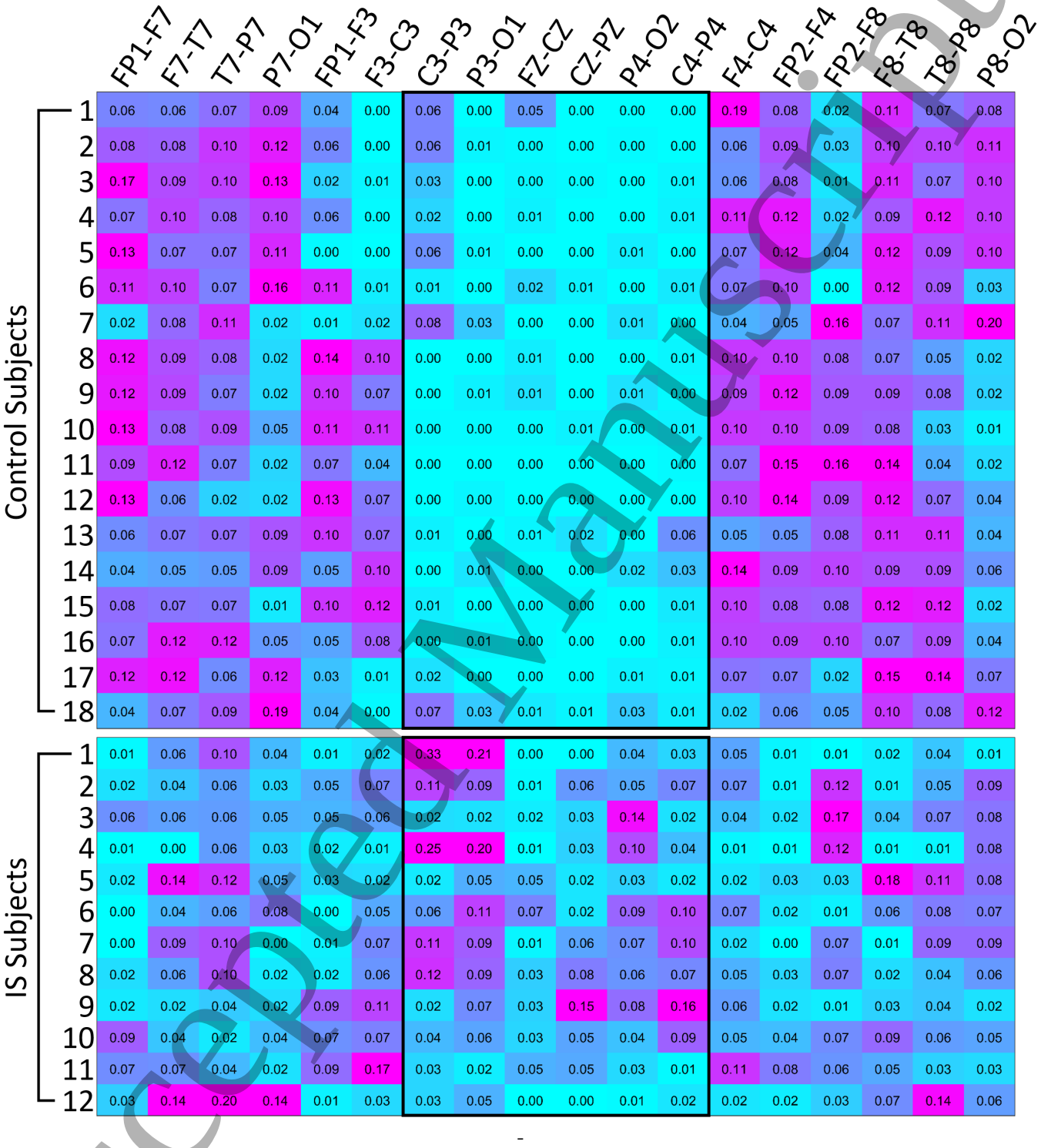

Fig 3. Normalized HFO Rates for Each Channel During Sleep. Each row represents a control or IS subject and each column corresponds to a channel from a longitudinal bipolar montage. HFO rates are normalized across each subject such that the sum of each row is 1.0, and higher rates appear pink while lower rates appear cyan. The channels contained in the black outlines correspond to posterior parasagittal areas.

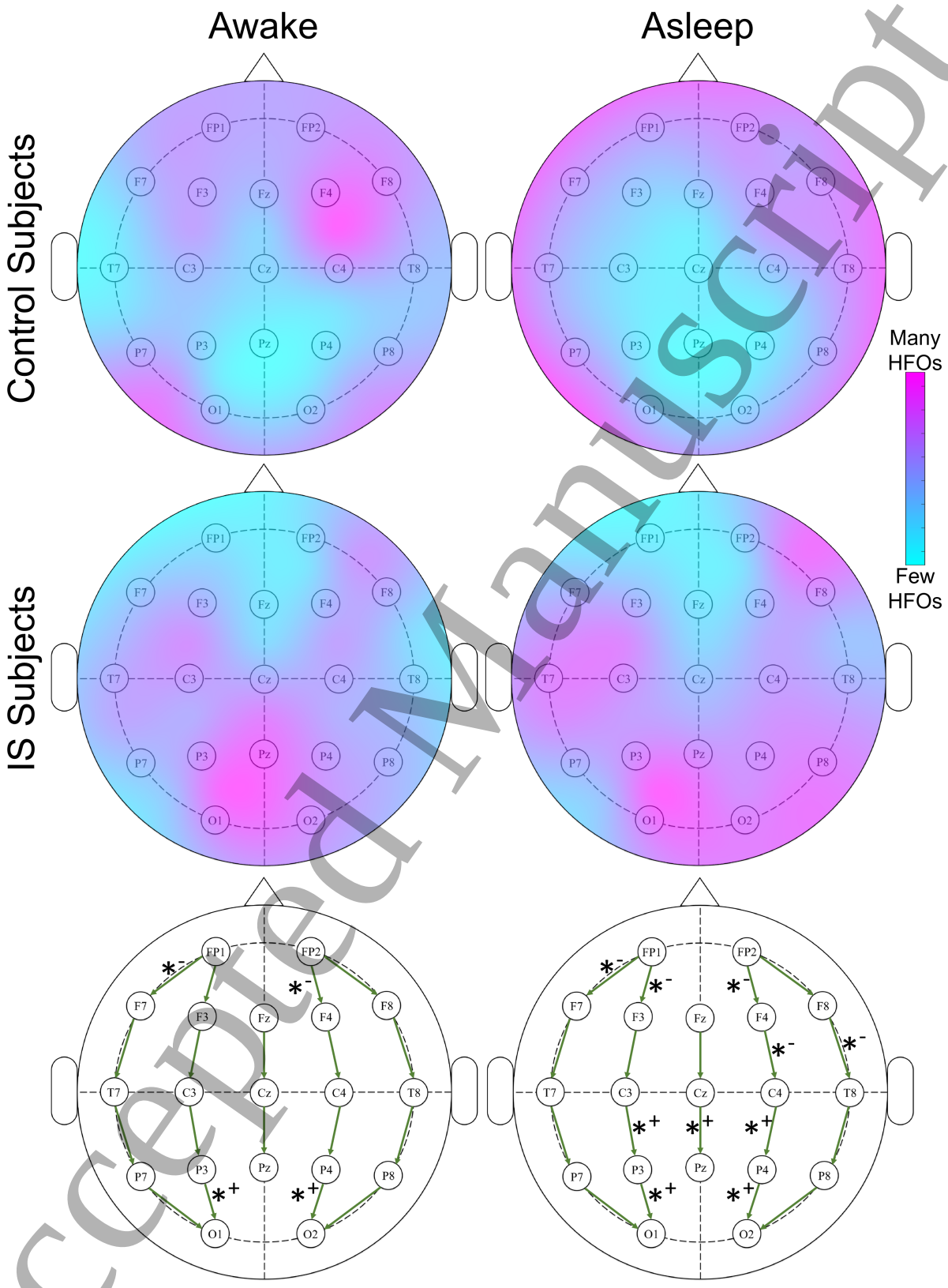

Fig 4. Median Spatial Distribution of HFOs Across Control and IS Subjects While Awake and Asleep. Areas in pink correspond to high HFO rates, and areas in cyan correspond to low HFO rates. The bottom plots demonstrate the longitudinal bipolar montage employed in this study, along with the channels that exhibited a significant increase ($*^{+}$) and decrease ($*^{-}$) in HFO rates in IS subjects compared to control subjects during wakefulness and sleep.

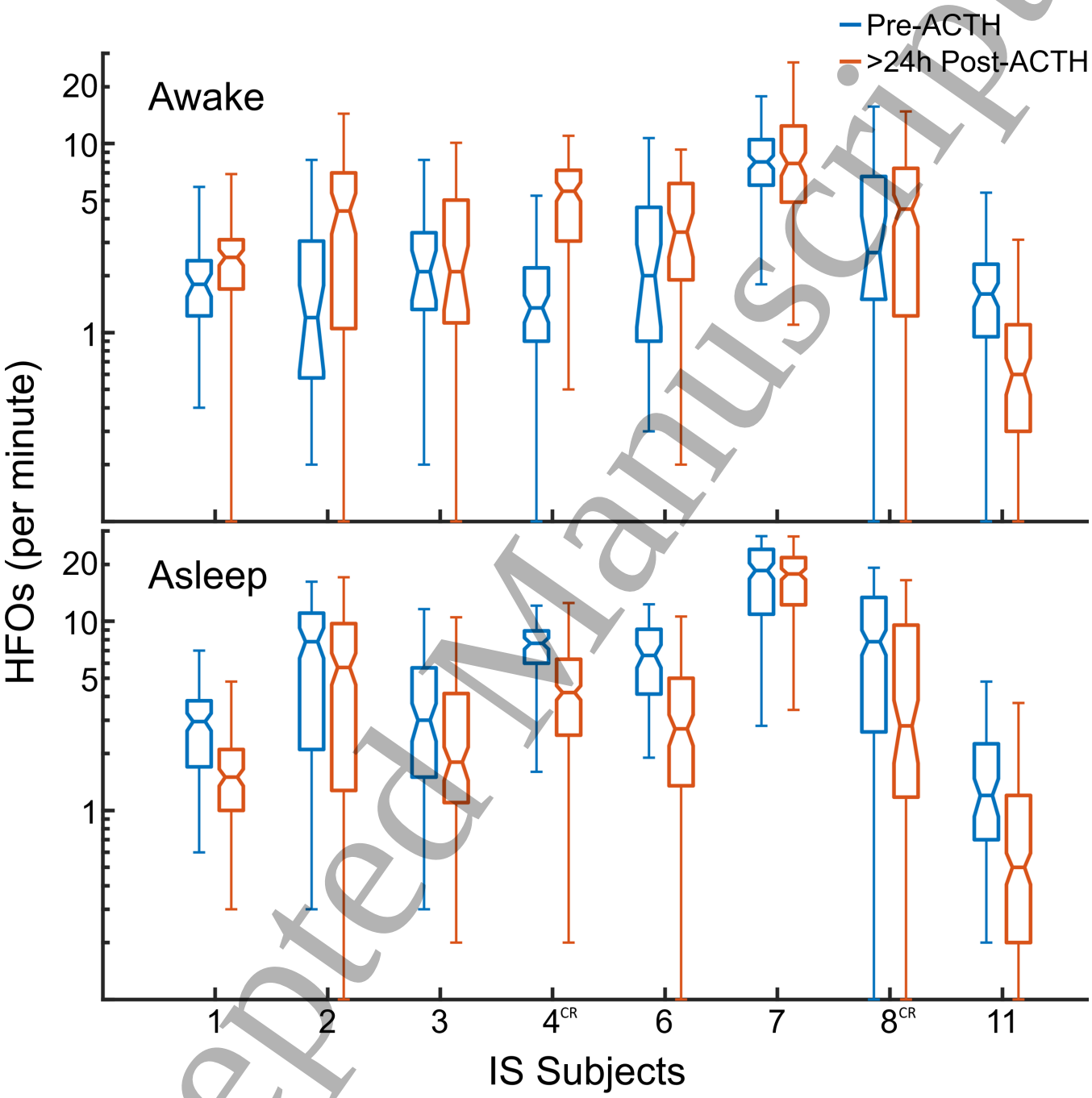

Fig 5. HFO Rates Before and After ACTH Initiation. HFOs during wakefulness (top) and sleep (bottom) before the start of ACTH therapy and at least 24 hours after it had been started were counted within multiple 10-minute intervals, and the distribution of HFO rates from these 10-minute intervals is depicted here. Note that a logarithmic y-axis scale is used for the box-and-whisker plots (interquartile range within box and all values within whiskers). Only IS Subjects underwent ACTH treatment during the study, and only eight out of twelve had sufficiently large pre- and post-ACTH study datasets for this analysis. IS Subjects 4 and 8 exhibited a clinical response (indicated by "CR") to ACTH therapy based on improvement in EEG and longitudinal follow-up.

data from controls that do not have epilepsy, but there are a few exceptions [61, 62].

Previous studies of interictal HFOs in scalp EEG relied on visual marking of events and exclusively used data collected during slow-wave sleep [26–28, 30, 31, 33, 38] or stage 2 sleep [32, 34]. This is the first report of HFO rates during wakefulness. In the most closely related study, Kobayashi et al. [38] found high rates of interictal scalp fast oscillations (41.0-140.6 Hz) in patients with West syndrome prior to treatment with ACTH. They reported a median ripple rate of approximately 7/minute in epilepsy patients and 0/min in healthy control subjects, which is similar to our median rates of 5.5/minute for IS patients and 0.98/minute for controls during sleep. They also found that ripples occurred most frequently in the P3-O1 and P4-O2 electrode pairs, consistent with our results. In that study, candidate HFOs were detected using automated time-frequency analysis, and the candidate events were visually reviewed to reject artifacts; 60 seconds of data were analyzed for each subject [38]. Given the significant differences in the amount of EEG data analyzed and the HFO detection methods, the consistency between our results and this prior study is noteworthy.

The visual validation of the automated HFO detection was accomplished by two independent human reviewers through manual classification of 1350 events from the control subjects and 1800 events from the IS subjects. This manual classification showed that the automated HFO detection is effective at identifying high-frequency artifacts and background EEG. However, the automated HFO detection had more difficulty distinguishing HFOs from high-frequency artifacts. This was likely related to the predetermined rejection cutoff values for voltage and line length that allowed some sharp transients and short muscle artifacts to escape rejection. For example, the sharp transient (row 2, column 1) and DC shift (row 2, column 2) from Supplementary Figure 3, as well as the short muscle artifact (row 4, column 1) from Supplementary Figure 4, were mis-identified as HFOs by the automated algorithm. The rest of the examples in these two figures were correctly identified by automated HFO detection. This is unlikely to affect the results of this study. In fact, we would expect even more of a relative difference between the HFO rates of control and IS subjects if the specificity in identifying HFOs was increased, since IS subjects had a proportionally larger number of true HFOs (51-59% vs 13-28%) in the signals classified as HFOs by the automated HFO detection. We should also note that even our trained reviewers had difficulty in agreeing on whether signals were true HFOs (75% concordance for control cases and 69% for IS cases), but this is not unexpected as previous studies have shown poor inter-rater reliability in manual identification of intracranial HFOs [63, 64].

In any study of fast oscillations using scalp EEG, the influence of muscle artifacts is particularly concerning. There are likely some brief muscle/ocular artifacts that escaped automated rejection, such as the one example previously described, in both the control and spasms subjects. However, these artifacts likely accounted for a small proportion of the total detected HFOs in the IS group, as this group exhibited substantially higher HFO rates during sleep when muscle/ocular movements (and their associated artifacts) are typically reduced. On the other hand, these artifacts likely comprised a more substantial proportion of the total detected HFOs in the control subjects, as HFOs were most prominent in artifact-prone EEG regions, e.g. the peripheral electrodes. Also note that, in this study, the vast majority of HFOs were likely interictal and not caused by muscle artifacts during clinical spasms, and there does not appear to be any clear association between the number of epileptic spasms and the HFO rates.

To further test the impact of muscle artifacts on HFO detection, we analyzed the EMG data from each subject. The results did not show an association between HFO rate and EMG power (Supplementary Figure 5, Kendall's Tau = 0.11), suggesting that the automatically detected HFOs are not significantly affected by EMG artifacts. Despite the difference in HFO rates between control subjects and IS subjects, their average EMG power was similar, and there was no statistical difference between the two groups during either wakefulness or sleep (Supplementary Figure 6). It should also be noted that both control subjects and IS subjects exhibited an expected and statistically significant decrease in EMG power during sleep compared to wakefulness, although this phenomenon seemed to be more pronounced in the control subjects (Supplementary Figure 6). It is possible that the IS subjects were intermittently awake during times when the sleep-wake classifier (mis)identified them as being asleep. In fact, some IS subjects had epileptic spasms throughout the night, even though epileptic spasms are not typically a phenomenon associated with sleep. However, it should be noted that control subjects' EMG power during sleep did not change significantly regardless of whether sleep staging was performed manually (by a trained polysomnographic technologist) or by the same automated algorithm that was used for the IS subjects (p =0.81 using a Wilcoxon signed-rank test); this was also true during wakefulness (p =0.21).

The occurrence of physiological ripples is an additional confounding factor. In previous studies, physiological HFOs were detected in the scalp EEG of healthy children and primarily occurred in the central and midline bipolar pairs [65, 66]. While, in these studies, rates varied widely across subjects, ripples occurred more frequently during light sleep and stage two sleep (stages N1 and N2), and approximately three-fourths of ripples co-occurred with sleep-specific transients [66]. Therefore, while false positive detections due to artifacts are less likely during sleep (due to reduced likelihood of muscle/ocular movements), there may be a simultaneous sleep-associated increase in true HFOs, leading to the overall lack of diurnal variation in the control subjects. This would likely occur in IS subjects, as well, but this effect appears to be masked by the overall higher rates of HFOs during sleep in this group. Note that the HFO rates reported in our study were not substantially affected by the manual versus automated sleep staging.

Spatially, HFOs in the control subjects were very infrequent in the posterior parasagittal region (bipolar channels C3-P3, P3-O1, Fz-Cz, Cz-Pz, P4-O2, C4-P4). In IS subjects, however, this was not the case, as a large portion of HFOs were detected from this region. In fact, overall, HFO rates in IS subjects were statistically increased in P3-O1 and P4-O2 during wakefulness when compared to control subjects, and statistically increased in C3-P3, P3-O1, CZ-PZ, P4-O2, and C4-P4 during sleep when compared to control subjects. These findings are consistent with a few prior studies that have suggested that interictal spikes and HFOs are predominantly phenomena of the posterior brain regions [38, 67]. It should be noted that in this study, the cortical areas of IS subjects with prominent discharges or hypsarrhythmia during EEG monitoring did not necessarily exhibit higher HFO rates. Further studies are needed to understand the electroneurophysiological etiology of these centro-posterior HFOs in IS patients, as well as the subgroup characteristics of the patients that exhibit this cortical phenomenon. Eventually, it may be possible to determine which patients are more or less likely to have infantile spasms based on the spatial distribution of their HFOs without the need for prolonged EEG monitoring.

In the 8 IS subjects with sufficient pre- and post-ACTH data, we observed a significant decrease in HFO rates during sleep after the start of ACTH therapy. Note that while this decrease in HFO rate became apparent within days of starting ACTH therapy, it may also persist with continued treatment [38]. No similar decrease was seen for IS subjects during wakefulness, although it is possible that not enough time had passed to observe this effect. There was also an abnormally low number of responders to ACTH treatment in this prospective cohort (4 out of 12, with two of these relapsing after initial treatment), based on an assessment of the presence of spasms and hypsarrhythmia on the EEG after two weeks. It is interesting to note that of the three subjects with the largest relative reduction in HFO rates after starting ACTH therapy, two of the three subjects (Subjects 4 and 8) subsequently responded clinically to the therapy. However, no conclusions can be drawn from this, given the low number of subjects and clinical responders, as statistically this outcome had an $\sim$11% chance of occurring by chance. Had we continued recording EEG for a longer period of time in patients receiving ACTH therapy, it is unknown if the reduction in HFO rate would have been even larger. For example, Zijlmans et al. [23] reported a reduction in HFOs with medical therapy and an increase in HFO rates when medication was reduced. Current thinking is that effective treatment should eliminate EEG evidence of epileptic spasms [68] and epileptiform discharges [69]; however, it is unknown if it is necessary for pathological HFOs to be completely eliminated. Future studies are required to determine the long-term effects of ACTH therapy on HFOs in IS patients. Many of the patients enrolled in this study have participated in serial longitudinal EEG monitoring at follow-up visits to help answer this question.

The current study has several limitations. Our analysis included only 12 subjects with IS, and a larger cohort would increase the power of the study. However, the subjects were prospectively recruited, and the large amount of data we analyzed for each subject increased the repeatability and robustness of the results. The fact that the IS cohort contained many patients that did not respond to treatment hindered our ability to analyze the effect of ACTH on HFO rate. Also, we were not able to perform manual sleep staging for the IS subjects (unlike for the control subjects), due to the disruption in typical sleep patterns [48–51]. However, we expect our automated wake/sleep classifier to have performed sufficiently for the IS subjects' datasets, given its 86% mean cross-validation accuracy for the control subjects and the assumption that sleep-wake features of EOG, EMG, ECG are consistent between control and IS subjects. Note that if the classifier performed at the level of random chance, we should expect no difference in the wakefulness/sleep characteristics, so as long as our classifier performed above chance level, the qualitative differences between wakefulness/sleep that were found in this study are real. In the future, it would also be useful to distinguish between the different stages of sleep for all subjects, as non-rapid eye movement (NREM) sleep is associated with

higher rates of HFOs compared to REM sleep or wakefulness [57, 70, 71] and may be less prone to muscle and eye-movement artifacts [72]. An additional limitation was that we analyzed the entire long-term EEG recording without accounting for the possible presence of epileptic spasms. However, we found through visual analysis that spasms were proportionally rare in our continuous, long-term data, and the majority of spasms were not associated with any detected HFOs. Lastly, we analyzed only HFOs in the ripple band (80-250 Hz), while there is evidence that fast ripples can also be detected in scalp EEG [31, 32]. Future studies should take steps to address these limitations.

Here we have provided deeper insight into the differences between control and IS subjects in HFO rate, diurnal variation, and spatial distribution, as well as changes in HFO rates with antiepileptic therapy using large datasets that are only analyzable using fully automated methods. Our results support computational analysis of noninvasive scalp HFOs as a robust and potentially valuable tool for the diagnosis and assessment of treatment response for epilepsy.

References

1. Pavone P, Striano P, Falsaperla R, Pavone L, Ruggieri M. Infantile spasms syndrome, West syndrome and related phenotypes: What we know in 2013. Brain and Development. 2014; 36(9):739–751.
2. Hrachovy RA, Frost JD. Infantile epileptic encephalopathy with hypsarrhythmia (infantile spasms/West syndrome). Journal of clinical neurophysiology : official publication of the American Electroencephalographic Society. 2003;20(6):408–25.
3. Pellock JM, Hrachovy R, Shinnar S, Baram TZ, Bettis D, Dlugos DJ, et al. Infantile spasms: A U.S. consensus report. Epilepsia. 2010; 51(10):2175–2189.
4. Riikonen RS. Favourable prognostic factors with infantile spasms. European Journal of Paediatric Neurology. 2010; 14(1):13–18.
5. Hussain SA. Treatment of infantile spasms. Epilepsia Open. 2018; 3(S2):143–154.
6. Wirrell EC, Nickels KC. Electroclinical Syndromes: Infantile Onset. In: Swaimann KF, Ashwal S, Ferriero DM, Schor NF, Finkel RS, Gropman AL, et al., editors. Swaiman's Pediatric Neurology. 6th ed. Elsevier; 2017. p. e1326–1345.
7. Lux AL, Osborne JP. A Proposal for Case Definitions and Outcome Measures in Studies of Infantile Spasms and West Syndrome: Consensus Statement of the West Delphi Group. Epilepsia. 2004; 45(11):1416–1428.
8. Caraballo RH, Fortini S, Reyes G, Carpio Ruiz A, Sanchez Fuentes SV, Ramos B. Epileptic spasms in clusters and associated syndromes other than West syndrome: A study of 48 patients. Epilepsy Research. 2016; 123:29–35.
9. Hrachovy RA, Frost JD, Kellaway P. Hypsarrhythmia: Variations on the Theme. Epilepsia. 1984; 25(3):317–325.
10. Donat JF, Lo WD. Asymmetric Hypsarrhythmia and Infantile Spasms in West Syndrome. Journal of Child Neurology. 1994; 9(3):290–296.
11. Hussain SA, Kwong G, Millichap JJ, Mytinger JR, Ryan N, Matsumoto JH, et al. Hypsarrhythmia assessment exhibits poor interrater reliability: A threat to clinical trial validity. Epilepsia. 2015; 56(1):77–81.
12. Mytinger JR, Hussain SA, Islam MP, Millichap JJ, Patel AD, Ryan NR, et al. Improving the inter-rater agreement of hypsarrhythmia using a simplified EEG grading scale for children with infantile spasms. Epilepsy Research. 2015; 116:93–98.
13. Crone NE, Sinai A, Korzeniewska A. High-frequency gamma oscillations and human brain mapping with electrocorticography. In: Progress in Brain Research. vol. 159; 2006. p. 275–295.
14. Smith MM, Weaver KE, Grabowski TJ, Rao RPN, Darvas F. Non-invasive detection of high gamma band activity during motor imagery. Frontiers in Human Neuroscience. 2014; 8.

15. Thürer B, Stockinger C, Focke A, Putze F, Schultz T, Stein T. Increased gamma band power during movement planning coincides with motor memory retrieval. NeuroImage. 2016; 125:172–181.

16. Zhang H, Fell J, Axmacher N. Electrophysiological mechanisms of human memory consolidation. Nature Communications. 2018; 9(1):4103.

17. Nowak M, Zich C, Stagg CJ. Motor Cortical Gamma Oscillations: What Have We Learnt and Where Are We Headed? Current Behavioral Neuroscience Reports. 2018; 5(2):136–142.

18. Kobayashi K, Oka M, Akiyama T, Inoue T, Abiru K, Ogino T, et al. Very Fast Rhythmic Activity on Scalp EEG Associated with Epileptic Spasms. Epilepsia. 2004; 45(5):488–496.

19. Iwatani Y, Kagitani-Shimono K, Tominaga K, Okinaga T, Kishima H, Kato A, et al. Ictal high-frequency oscillations on scalp EEG recordings in symptomatic West syndrome. Epilepsy Research. 2012; 102(1-2):60–70.

20. Kobayashi K, Miya K, Akiyama T, Endoh F, Oka M, Yoshinaga H, et al. Cortical contribution to scalp EEG gamma rhythms associated with epileptic spasms. Brain and Development. 2013; 35(8):762–770.

21. Jiruska P, Alvarado-Rojas C, Schevon CA, Staba R, Stacey W, Wendling F, et al. Update on the mechanisms and roles of high-frequency oscillations in seizures and epileptic disorders. Epilepsia. 2017; 58(8):1330–1339.

22. Wu JY, Koh S, Sankar R, Mathern GW. Paroxysmal fast activity: An interictal scalp EEG marker of epileptogenesis in children. Epilepsy Research. 2008; 82(1):99–106.

23. Zijlmans M, Jacobs J, Zelmann R, Dubeau F, Gotman J. High-frequency oscillations mirror disease activity in patients with epilepsy. Neurology. 2009; 72(11):979–986.

24. Andrade-Valenca LP, Dubeau F, Mari F, Zelmann R, Gotman J. Interictal scalp fast oscillations as a marker of the seizure onset zone. Neurology. 2011; 77(6):524–531.

25. Jacobs J, Zijlmans M, Zelmann R, Chatillon CÉ, Hall J, Olivier A, et al. High-frequency electroencephalographic oscillations correlate with outcome of epilepsy surgery. Annals of Neurology. 2010; 67(2):209–220.

26. Kuhnke N, Schwind J, Dümpelmann M, Mader M, Schulze-Bonhage A, Jacobs J. High Frequency Oscillations in the Ripple Band (80–250 Hz) in Scalp EEG: Higher Density of Electrodes Allows for Better Localization of the Seizure Onset Zone. Brain Topography. 2018; 31(6):1059–1072.

27. Melani F, Zelmann R, Dubeau F, Gotman J. Occurrence of scalp-fast oscillations among patients with different spiking rate and their role as epileptogenicity marker. Epilepsy Research. 2013; 106(3):345–356.

28. von Ellenrieder N, Andrade-Valença LP, Dubeau F, Gotman J. Automatic detection of fast oscillations (40–200Hz) in scalp EEG recordings. Clinical Neurophysiology. 2012; 123(4):670–680.

29. Zelmann R, Lina JM, Schulze-Bonhage A, Gotman J, Jacobs J. Scalp EEG is not a Blur: It Can See High Frequency Oscillations Although Their Generators are Small. Brain Topography. 2014; 27(5):683–704.

30. Kuhnke N, Klus C, Dümpelmann M, Schulze-Bonhage A, Jacobs J. Simultaneously recorded intracranial and scalp high frequency oscillations help identify patients with poor postsurgical seizure outcome. Clinical Neurophysiology. 2019; 130(1):128–137.

31. Pizzo F, Frauscher B, Ferrari-Marinho T, Amiri M, Dubeau F, Gotman J. Detectability of Fast Ripples (>250 Hz) on the Scalp EEG: A Proof-of-Principle Study with Subdermal Electrodes. Brain Topography. 2016; 29(3):358–367.

32. Bernardo D, Nariai H, Hussain SA, Sankar R, Salamon N, Krueger DA, et al. Visual and semi-automatic non-invasive detection of interictal fast ripples: A potential biomarker of epilepsy in children with tuberous sclerosis complex. Clinical Neurophysiology. 2018; 129(7):1458–1466.

33. Kramer MA, Ostrowski LM, Song DY, Thorn EL, Stoyell SM, Parnes M, et al. Scalp recorded spike ripples predict seizure risk in childhood epilepsy better than spikes. Brain. 2019; 142(5):1296–1309.

34. Gong P, Xue J, Qian P, Yang H, Liu X, Cai L, et al. Scalp-recorded high-frequency oscillations in childhood epileptic encephalopathy with continuous spike-and-wave during sleep with different etiologies. Brain and Development. 2018; 40(4):299–310.

35. Cao D, Chen Y, Liao J, Nariai H, Li L, Zhu Y, et al. Scalp EEG high frequency oscillations as a biomarker of treatment response in epileptic encephalopathy with continuous spike-and-wave during sleep (CSWS). Seizure. 2019; 71:151–157.

36. Kobayashi K, Yoshinaga H, Toda Y, Inoue T, Oka M, Ohtsuka Y. High-frequency oscillations in idiopathic partial epilepsy of childhood. Epilepsia. 2011; 52(10):1812–1819.

37. Kobayashi K, Ohuchi Y, Shibata T, Hanaoka Y, Akiyama M, Oka M, et al. Detection of fast (40–150 Hz) oscillations from the ictal scalp EEG data of myoclonic seizures in pediatric patients. Brain and Development. 2018; 40(5):397–405.

38. Kobayashi K, Akiyama T, Oka M, Endoh F, Yoshinaga H. A storm of fast (40-150Hz) oscillations during hypsarrhythmia in West syndrome. Annals of Neurology. 2015; 77(1):58–67.

39. Charupanit K, Nunez MD, Bernardo D, Bebin M, Krueger DA, Northrup H, et al. Automated Detection of High Frequency Oscillations in Human Scalp Electroencephalogram. In: 2018 40th Annual International Conference of the IEEE Engineering in Medicine and Biology Society (EMBC). IEEE; 2018. p. 3116–3119.

40. Nariai H, Beal J, Galanopoulou AS, Mowrey WB, Bickel S, Sogawa Y, et al. Scalp EEG Ictal gamma and beta activity during infantile spasms: Evidence of focality. Epilepsia. 2017; 58(5):882–892.

41. Kobayashi K, Akiyama T, Oka M, Endoh F, Yoshinaga H. Fast (40–150Hz) oscillations are associated with positive slow waves in the ictal EEGs of epileptic spasms in West syndrome. Brain and Development. 2016; 38(10):909–914.

42. Sparrow SS, Cicchetti DV, Saulnier CA. Vineland Adaptive Behavior Scales, Third Edition. 3rd ed. San Antonio, TX: Pearson; 2016.

43. Jasper HH. Report of the committee on methods of clinical examination in electroencephalography. Electroencephalography and Clinical Neurophysiology. 1958; 10(2):370–375.

44. Millett D, Stern JM. Fundamentals of EEG. In: Sirven JI, Stern JM, editors. Atlas of Video-EEG Monitoring. McGraw-Hill; 2011. p. 680.

45. Charupanit K, Lopour BA. A Simple Statistical Method for the Automatic Detection of Ripples in Human Intracranial EEG. Brain Topography. 2017; 30(6):724–738.

46. Burnos S, Hilfiker P, Sürücü O, Scholkmann F, Krayenbühl N, Grunwald T, et al. Human Intracranial High Frequency Oscillations (HFOs) Detected by Automatic Time-Frequency Analysis. PLoS ONE. 2014; 9(4):e94381.

47. Britton JW, Frey LC, Hopp JL, Korb P, Koubeissi MZ, Lievens WE, et al. Appendix 4. Common Artifacts During EEG Recording. In: Louis EKS, Frey LC, editors. Electroencephalography (EEG): An Introductory Text and Atlas of Normal and Abnormal Findings in Adults, Children, and Infants. Chicago: American Epilepsy Society; 2016.

48. Hrachovy RA, Frost JD, Kellaway P. Sleep characteristics in infantile spasms. Neurology. 1981; 31(6):688–688.

49. Kellaway P. Sleep and Epilepsy. Epilepsia. 1985; 26(s1):S15–S30.

50. Altunel A, Sever A, Altunel EÖ. Hypsarrhythmia paroxysm index: A tool for early prediction of infantile spasms. Epilepsy Research. 2015; 111:54–60.

51. Altunel A, Altunel EÖ, Sever A. The Utility of the Hypsarrhythmia Paroxysm Index and Sleep Spindles in EEG for Predicting Cognitive Outcomes in a Case Series of Infantile Spasms. Journal of Neurology & Neurophysiology. 2015; 06(05).

52. Fisher RA. The Use of Multiple Measurements in Taxonomic Problems. Annals of Eugenics. 1936; 7(2):179–188.

53. Mann HB, Whitney DR. On a Test of Whether one of Two Random Variables is Stochastically Larger than the Other. The Annals of Mathematical Statistics. 1947; 18(1):50–60.

54. Wilcoxon F. Individual Comparisons by Ranking Methods. Biometrics Bulletin. 1945; 1(6):80.

55. Dümpelmann M, Jacobs J, Schulze-Bonhage A. Temporal and spatial characteristics of high frequency oscillations as a new biomarker in epilepsy. Epilepsia. 2015; 56(2):197–206.

56. Clemens Z, Molle M, Eross L, Barsi P, Halasz P, Born J. Temporal coupling of parahippocampal ripples, sleep spindles and slow oscillations in humans. Brain. 2007; 130(11):2868–2878.

57. Staba RJ, Wilson CL, Bragin A, Jhung D, Fried I, Engel J. High-frequency oscillations recorded in human medial temporal lobe during sleep. Annals of Neurology. 2004; 56(1):108–115.

58. Schevon CA, Trevelyan AJ, Schroeder CE, Goodman RR, McKhann G, Emerson RG. Spatial characterization of interictal high frequency oscillations in epileptic neocortex. Brain. 2009; 132(11):3047–3059.

59. Liu S, Sha Z, Sencer A, Aydoseli A, Bebek N, Abosch A, et al. Exploring the time–frequency content of high frequency oscillations for automated identification of seizure onset zone in epilepsy. Journal of Neural Engineering. 2016; 13(2):026026.

60. Bagshaw AP, Jacobs J, LeVan P, Dubeau F, Gotman J. Effect of sleep stage on interictal high-frequency oscillations recorded from depth macroelectrodes in patients with focal epilepsy. Epilepsia. 2009; 50(4):617–628.

61. Gliske SV, Irwin ZT, Chestek C, Hegeman GL, Brinkmann B, Sagher O, et al. Variability in the location of high frequency oscillations during prolonged intracranial EEG recordings. Nature Communications. 2018; 9(1):2155.

62. Liu S, Gurses C, Sha Z, Quach MM, Sencer A, Bebek N, et al. Stereotyped high-frequency oscillations discriminate seizure onset zones and critical functional cortex in focal epilepsy. Brain. 2018; 141(3):713–730.

63. Spring AM, Pittman DJ, Aghakhani Y, Jirsch J, Pillay N, Bello-Espinosa LE, et al. Interrater reliability of visually evaluated high frequency oscillations. Clinical Neurophysiology. 2017; 128(3):433–441.

64. Spring AM, Pittman DJ, Aghakhani Y, Jirsch J, Pillay N, Bello-Espinosa LE, et al. Generalizability of High Frequency Oscillation Evaluations in the Ripple Band. Frontiers in Neurology. 2018; 9.

65. Mooij AH, Raijmann RCMA, Jansen FE, Braun KPJ, Zijlmans M. Physiological Ripples (± 100 Hz) in Spike-Free Scalp EEGs of Children With and Without Epilepsy. Brain Topography. 2017; 30(6):739–746.

66. Mooij AH, Frauscher B, Goemans SAM, Huiskamp GJM, Braun KPJ, Zijlmans M. Ripples in scalp EEGs of children: co-occurrence with sleep-specific transients and occurrence across sleep stages. Sleep. 2018; 41(11).

67. Oka M, Kobayashi K, Akiyama T, Ogino T, Oka E. A study of spike-density on EEG in West syndrome. Brain and Development. 2004; 26(2):105–112.

68. Yamada K, Toribe Y, Kimizu T, Kimura S, Ikeda T, Mogami Y, et al. Predictive value of EEG findings at control of epileptic spasms for seizure relapse in patients with West syndrome. Seizure. 2014; 23(9):703–707.

69. Hayashi Y, Yoshinaga H, Akiyama T, Endoh F, Ohtsuka Y, Kobayashi K. Predictive factors for relapse of epileptic spasms after adrenocorticotropic hormone therapy in West syndrome. Brain and Development. 2016; 38(1):32–39.

70. Jirsch JD. High-frequency oscillations during human focal seizures. Brain. 2006; 129(6):1593–1608.

71. Sakuraba R, Iwasaki M, Okumura E, Jin K, Kakisaka Y, Kato K, et al. High frequency oscillations are less frequent but more specific to epileptogenicity during rapid eye movement sleep. Clinical Neurophysiology. 2016; 127(1):179–186.

72. von Ellenrieder N, Beltrachini L, Perucca P, Gotman J. Size of cortical generators of epileptic interictal events and visibility on scalp EEG. NeuroImage. 2014; 94:47–54.